Biochem. J. (1992) 283, 265–272 (Printed in Great Britain)

Gluconeogenesis stimulated by extracellular ATP is triggered by the initial increase in the intracellular Ca^{2+} concentration of the periphery of hepatocytes

Masahiko KOIKE, Tadashi KASHIWAGURA* and Noriaki TAKEGUCHI
Faculty of Pharmaceutical Sciences, Toyama Medical and Pharmaceutical University, Toyama, 930-01 Japan

Extracellular ATP, ADP and GTP increased the intracellular free Ca^{2+} concentration ($[Ca^{2+}]_i$) in a suspension of isolated rat hepatocytes. The $[Ca^{2+}]_i$ was determined by measuring fura-2 fluorescence, and its increase was biphasic. The initial transient rise was followed by a longer-lasting plateau. The peak of the early component preceded the plateau level of the second component. A time course of change in $[Ca^{2+}]_i$ in single cells at 100 μM-ATP was very similar to that observed in the suspension system. Preincubation of hepatocytes with 40 mM-caffeine, 2 mM-oxalate or 60 μM-dantrolene sodium inhibited the P_2 purinergic response. The plateau phase was not observed when measured in the presence of extracellular 100 μM-$LaCl_3$ or in the absence of extracellular Ca^{2+}. The distribution of $[Ca^{2+}]_i$ in single hepatocytes was also determined by fluorescence image analysis. In the initial phase, the increase in $[Ca^{2+}]_i$ is greater in the peripheral region than the central region of the cell. Degradation of extracellular ATP by ecto-ATPase in the hepatocyte suspension was measured; the amount of ATP degradation was less than 10–15% of the initial amount (100 μM) during the measurement of the intracellular $[Ca^{2+}]_i$ in the cell suspension. Extracellular ATP stimulated glucose synthesis. The rate of glucose production also showed two components, the initial fast component within 1 min and the subsequent slower component. The rate of the initial fast component did not depend on the presence or absence of extracellular Ca^{2+}, whereas the rate of the subsequent component depended on it. The present study shows that the initial transient rise in $[Ca^{2+}]_i$ plays an important role in triggering the gluconeogenesis.

INTRODUCTION

Extracellular ATP and related substances are released from several different types of cells, such as platelets and neurons. Extracellular ATP interacts with specific receptors (purinergic receptors) on the surface of many different cells and influences their biological processes [1]. In hepatocytes and perfused livers, the extracellular ATP stimulates glycogenolysis [2–7], gluconeogenesis [8] and ureagenesis [9]. These effects of extracellular ATP are suggested to be mediated by increases in the intracellular free Ca^{2+} concentration ($[Ca^{2+}]_i$) through breakdown of phospholipids, generation of inositol trisphosphate and diacylglycerol [8,10–13].

In the present study we measured the time course of change in $[Ca^{2+}]_i$ of isolated rat hepatocytes and the rate of gluconeogenesis that were stimulated by extracellular ATP. The rapid initial increase in $[Ca^{2+}]_i$ occurred in the peripheral region (not the central region) of the cell, and it was due to mobilization from intracellular Ca^{2+} pools. The rate of gluconeogenesis in the initial period also increased, indicating that the initial rise in the peripheral $[Ca^{2+}]_i$ is a very important event for triggering the gluconeogenesis.

MATERIALS AND METHODS

Preparation of isolated hepatocytes

Isolated hepatocytes were prepared by the method of Berry & Friend [14] with modifications [15] from 48 h-starved male rats of the Wistar strain, weighing 200–250 g. Cell viability, judged by Trypan Blue exclusion, was more than 90%. Isolated hepatocytes were suspended in Krebs–Henseleit solution [16] supplemented with 2% (w/v) BSA (Fraction V). The suspension of cells was stored on ice with gentle shaking under an O_2/CO_2 (19:1) atmosphere and used within 6 h.

Fura-2 loading

Hepatocytes were preincubated in Krebs–Henseleit solution for 10 min at 37 °C under O_2/CO_2 (19:1). Fura-2 loading was started by addition of 45 μl of 1 mM-fura-2 AM (solubilized in dimethyl sulphoxide) and 6 μl of 25% (w/v) Pluronic F127 (in dimethyl sulphoxide) to 6 ml of the hepatocyte suspension (3.3×10^6 cells/ml). The suspension was incubated for 30 min at 37 °C. The cells were then washed twice in the ice-cold solution and resuspended in 6 ml of Krebs–Henseleit solution containing 2% BSA. The cell suspension was stored on ice until use. After loading, the intracellular fura-2 concentration was found to be 200–400 μM. The value was determined from the amount of fura-2 released from the cells after treatment with 0.1% Triton X-100. The autofluorescence of unloaded cells was less than 20% of the signal of dye-loaded cells.

Measurement of $[Ca^{2+}]_i$ in cell suspension

Hepatocytes loaded with fura-2 were resuspended into a modified Ca^{2+}-free Krebs–Henseleit solution containing 20 mM-Hepes in exchange for bicarbonate, pH 7.4 (3.3×10^5 cells/ml, i.e. 0.37 mg dry wt./ml). A 3 ml portion of the cell suspension was transferred to a quartz cuvette placed in a thermostatically controlled sample compartment of a dual-excitation-wavelength spectrofluorimeter (Spex Fluorolog-2). To the cell suspension, 1.3 mM-$CaCl_2$ or 0.5 mM-EGTA was added. The cells were

Abbreviations used: $[Ca^{2+}]_i$, intracellular free Ca^{2+} concentration; fura-2 AM, 1-[2-(5'-carboxyoxazol-2'-yl)-6-aminobenzofuran-5-oxy]-2-(2'-amino-5'-methylphenoxy)ethane-*NNN'N'*-tetra-acetic acid, penta-acetoxymethyl ester; SR, sarcoplasmic reticulum; ER, endoplasmic reticulum; ATP[S], adenosine 5'-[γ-thio]triphosphate.

* To whom correspondence should be addressed. Present address: Department of Biological Science and Technology, Faculty of Engineering, Aomori University, Aomoro 030, Japan.

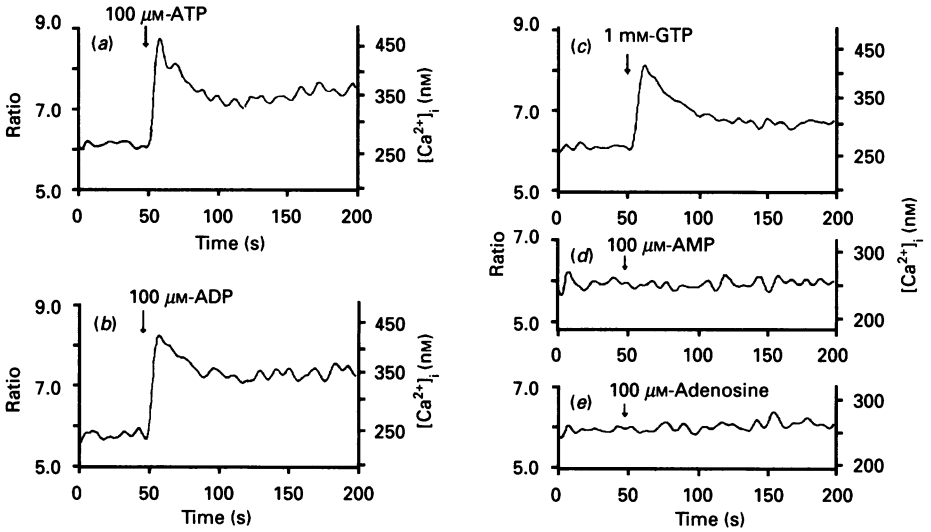

Fig. 1. Effects of purine nucleotides on the $[Ca^{2+}]_i$ and the ratio of 340 nm/380 nm fura-2 fluorescence

The methods for preparation of fura-2-loaded hepatocytes and the measurement of fura-2-dependent fluorescence ratio were described in the Materials and methods section. Typical examples in the presence of 1.3 mM-Ca^{2+} in the cell suspension medium are presented. Agonist at the indicated concentrations was added at the arrow: (*a*) ATP, (*b*) ADP, (*c*) GTP, (*d*) AMP and (*e*) adenosine.

warmed at 25 °C with stirring for 5 min before measurements. Fluorescence were measured at excitation wavelengths of 340 nm and 380 nm and an emission wavelength of 505 nm. Since the intracellular fluorescence of fura-2 decreased rapidly at 37 °C, probably owing to the dye leakage or its active extrusion, we measured $[Ca^{2+}]_i$ at 25 °C. According to our preliminary experiments, characteristics of the hormone-induced $[Ca^{2+}]_i$ transients at 37 °C were similar to those at 25 °C. At the end of experiment, fluorescence at the two excitation wavelengths was measured after addition of 5 mM-EGTA for correction of dye leakage. The ratio of fluorescence intensity excited at 340 nm/380 nm and $[Ca^{2+}]_i$ were calculated as described elsewhere [17–19].

Measurement of $[Ca^{2+}]_i$ distribution in single hepatocytes

Fura-2-loaded hepatocytes were placed on a thin glass slide, which was set as the bottom glass of a chamber (Japan Spectroscopic, SC-20) with 400 μl of the Hepes-buffered Krebs–Henseleit solution. A Nikon TMD-EFQ inverted microscope was used. For bright-field pictures, a Nomarski optical system was used. Fluorescence images were obtained at excitation wavelengths of 340 and 380 nm with an emission wavelength of 510 nm (interference filter) and digitized at 8-bit resolution and analysed with an IM1 image-analysis system (SPEX, Edison, NJ, U.S.A.). After corrections for background fluorescence and camera uniformity, the intensity ratio (340 nm/380 nm) was calculated and $[Ca^{2+}]_i$ was obtained as previously described [18].

Measurement of $[Ca^{2+}]_i$ in single hepatocytes

Fura-2-loaded hepatocytes were observed under the microscope as described above for the measurement of $[Ca^{2+}]_i$ distribution in single hepatocytes. The total fluorescence intensity from one single cell was monitored by using a photon-counting technique (Spex Fluorog-2 spectrofluorimeter). The background noise was calibrated.

Measurement of gluconeogenesis in hepatocytes

Isolated hepatocytes were incubated in Krebs–Henseleit solution containing 2% BSA with constant shaking (100–110 times/min) at 37 °C. The incubation gas phase was O_2/CO_2 (19:1). Hepatocytes (about 4.3 mg dry wt./ml of cells) were preincubated with 4 mM-glutamine for 10 min. Then ATP, ADP or GTP was added to the medium for stimulation of glucose production. At predetermined times, the metabolic reaction was stopped by addition of $HClO_4$ to a final concentration of 4% (w/v). Then the sample solution was centrifuged to remove insoluble material. The supernatant was neutralized with 2 M-K_2CO_3/0.58 M-triethanolamine and used for assay of glucose. The dry weight of the cell suspension was determined for each preparation. A factor of 3.5 was used to convert the dry wt. into the wet wt. of cells [20]. Glucose was measured enzymically by the method of Bergmeyer *et al.* [21]. The amount of glucose produced in the preincubation process was subtracted from the total amount of synthesis.

Measurement of ATP hydrolysis of ecto-ATPase in hepatocyte suspension

The amount of ATP degradation by membrane-bound ecto-ATPase was measured. Hepatocytes at various cell populations were preincubated for 5 min under the same conditions as described above, and then 100 μM-ATP was added. After 3 min, the cell was separated by centrifugation and the metabolic reaction in the supernatant was rapidly stopped by the addition of $HClO_4$ to a final concentration of 4%. The concentration of ATP in the neutralized $HClO_4$ extract was measured enzymically by the method of Lamprecht & Trautschold [22].

Reagents

Fura-2 AM, Pluronic F127 and Hepes were obtained from Dojindo Laboratories Co. (Kumamoto, Japan). ATP, ADP and AMP were from Oriental Yeast Co. (Tokyo, Japan). Adenosine, phenylephrine and vasopressin were from Sigma Chemical Co. GTP and adenosine 5′-[γ-thio]triphosphate (ATP[S]) were from Boehringer Mannheim Co. Dibutyryl cyclic AMP was from Daiichi Seiyaki Co. (Tokyo, Japan). Dantrolene sodium was obtained from Yamanouchi Pharmaceutical Co. (Tokyo, Japan).

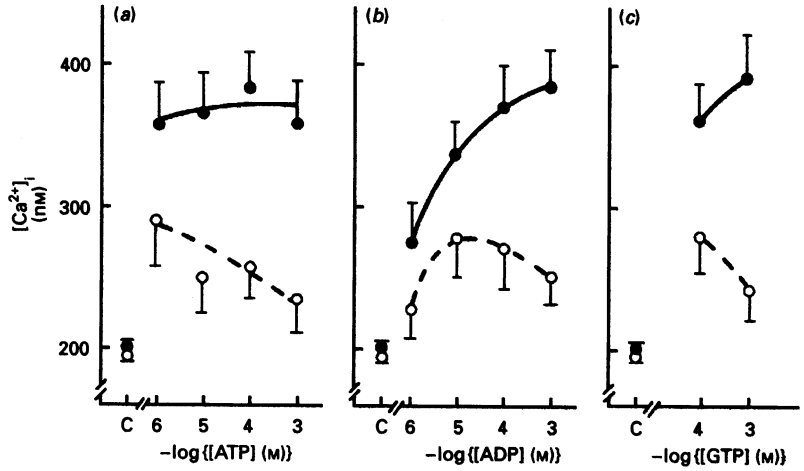

Fig. 2. Initial transient and plateau $[Ca^{2+}]_i$ levels as a function of agonist concentrations

The transient (●) and plateau $[Ca^{2+}]_i$ (○) were measured 7 s and 100 s after stimulation with agonist respectively: (*a*) ATP, (*b*) ADP and (*c*) GTP. Data are means ± S.E.M. from 6–8 different cell preparations. Control values in the absence of agonist are also shown (C).

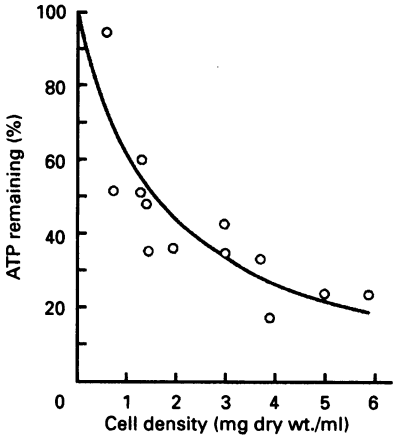

Fig. 3. Degradation of extracellular ATP by ecto-ATPase

Hepatocytes were preincubated for 5 min at various cell densities as described in the Materials and methods section. Then 100 μM-ATP was added and incubated for 3 min. After separating the cells, the metabolic reaction in the supernatant was rapidly stopped by addition of $HClO_4$ and the ATP concentration was measured.

RESULTS

Effects of purine nucleotides on $[Ca^{2+}]_i$

Figs. 1(*a*)–1(*c*) show that 100 μM-ATP, 100 μM-ADP and 1 mM-GTP cause increases in $[Ca^{2+}]_i$ of the isolated hepatocytes measured in the cell suspension in the presence of 1.3 mM-Ca^{2+}. The increase consists of the initial rapid transient peak component and the long-lasting (plateau) component. The transient rise was observed within 1 s after the addition of the nucleotide, and its peak was attained within about 7 s. The basal level of $[Ca^{2+}]_i$ was 198 ± 4 nM (n = 22). The peak levels were 384 ± 26 nM (n = 8), 372 ± 30 nM (n = 7) and 393 ± 33 nM (n = 7) measured 7 s after the addition of ATP, ADP and GTP respectively. Plateau levels were reached within 100 s, and the $[Ca^{2+}]_i$ values were 258 ± 23 nM (n = 8), 272 ± 30 nM (n = 7) and 244 ± 23 nM (n = 7) (at 100 s) respectively (Figs. 1*a*–1*c*). In contrast with ATP, ADP and GTP, application of 0.1 mM-AMP or -adenosine did not induce change in $[Ca^{2+}]_i$ (Figs. 1*d* and 1*e*).

In Fig. 2, values of transient peak and plateau levels (at 7 s and 100 s) of $[Ca^{2+}]_i$ are plotted against concentrations of applied purinergic agonists.

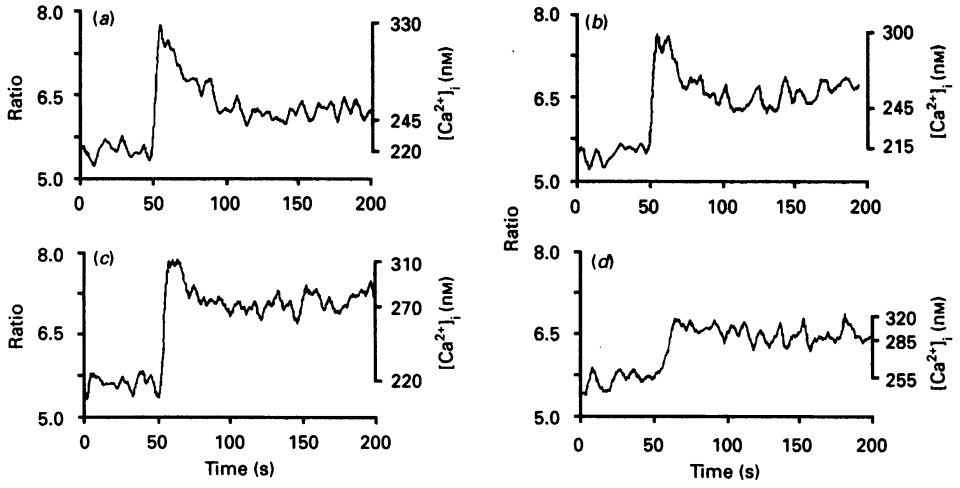

Fig. 4. Effects of ATP[S] on the $[Ca^{2+}]_i$ and the ratio of 340 nm/380 nm fura-2 fluorescence

Experimental procedures were described in the Materials and methods section. Typical examples in the presence of 1.3 mM-Ca^{2+} in the cell suspension medium are presented. ATP[S] at various concentrations was added at 50 s: (*a*) 1000 μM, (*b*) 100 μM, (*c*) 10 μM, (*d*) 1 μM.

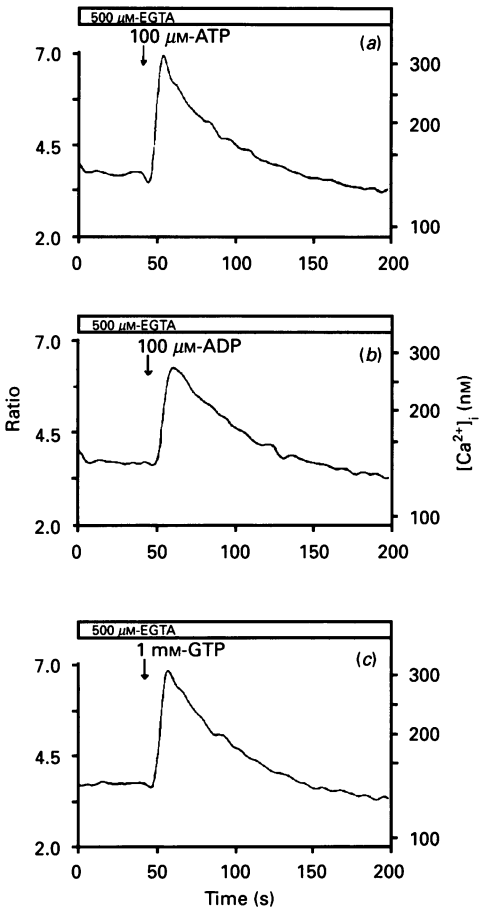

Fig. 5. Effects of extracellular Ca^{2+} on ATP^-, ADP^- and GTP-dependent changes in $[Ca^{2+}]_i$

Typical results stimulated by 100 μM-ATP (*a*), 100 μM-ADP (*b*) and 1 mM-GTP (*c*) in the absence of extracellular Ca^{2+} in the cell-suspension medium are shown. The horizontal bar at the top represents the duration of application of 500 μM-EGTA.

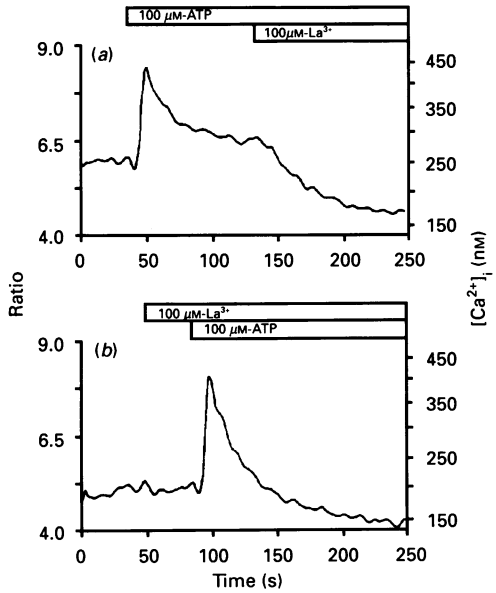

Fig. 6. Effects of 100 μM-La^{3+} on $[Ca^{2+}]_i$ in the presence of 1.3 mM extracellular Ca^{2+} under stimulation with 100 μM-ATP

Typical results are shown. $[Ca^{2+}]_i$ was measured in cell suspensions.

Table 1. Effects of various inhibitors on the initial transient increase in $[Ca^{2+}]_i$ induced by extracellular purinergic agonists

Data were obtained 50 s after the addition of agonists in the presence of 0.5 mM-EGTA. Hepatocytes were pretreated for 30–40 min with either 40 mM-caffeine or 60 μM-dantrolene sodium or for 15 min with 2 mM-oxalate, and then stimulated with agonists. Results were expressed as means ± S.E.M. (number of preparations) as percentages of the control value (100 %).

	$[Ca^{2+}]_i$ (% of each control)		
Inhibitor	ATP	ADP	GTP
None (EGTA)	102.6 ± 14.3 (3)	94.0 ± 12.9 (3)	97.2 ± 2.1 (3)
40 mM-Caffeine	47.8 ± 2.4 (5)	36.5 ± 1.9 (5)	37.0 ± 4.8 (5)
2 mM-Oxalate	56.6 ± 4.4 (4)	59.8 ± 8.7 (4)	47.6 ± 4.9 (3)
60 μM-Dantrolene	26.5 ± 3.0 (6)	25.0 ± 3.5 (7)	25.6 ± 4.6 (5)

ATP degradation by ecto-ATPase

It was previously reported that extracellular ATP is hydrolysed by ecto-ATPase in the hepatocyte plasma membrane [23,24]. We measured degradation of extracellular ATP by ecto-ATPase of isolated hepatocytes (Fig. 3). Fig. 3 shows the remaining amount of ATP in the cell suspension after a 3 min incubation as a function of cell density in the medium. Its initial ATP concentration was 100 μM. In this report, we used three different cell densities, about 0.37 mg dry wt./ml for measuring $[Ca^{2+}]_i$ in cell suspensions, 0.03 mg dry wt./ml for measuring $[Ca^{2+}]_i$ in single cells and about 4.3 mg dry wt./ml for measuring glucose production. In the experiments at 100 μM-ATP (Figs. 1, 5 and 6), the actual ATP concentration in the cell suspension after the 3 min incubation is speculated to be 85–90 % of the initial value, and this decrease in the ATP concentration may have not induced significant errors in the results. When the initial ATP concentration is less than 100 μM, a substantial amount of ATP may be degraded. Similarly, ADP and GTP may also be degraded by ecto-nucleotidases. Therefore, the results shown in Fig. 2 measured at 1 μM and 10 μM nucleotides may include some error.

Fig. 4 shows changes in $[Ca^{2+}]_i$ in the hepatocyte suspension stimulated by 1 μM, 10 μM, 100 μM- and 1000 μM-ATP[S], which is an ATP analogue poorly hydrolysed by ecto-ATPase. The initial peak values did not depend on the ATP[S] concentration, and the plateau values increased as the ATP[S] concentration decreased. These findings with ATP[S] in the concentration range from 1 to 1000 μM are in agreement with the results obtained with ATP shown in Fig. 2, indicating that the results in Fig. 2 are at least qualitatively correct.

Effects of Ca^{2+} elimination from the extracellular medium on the two components of the $[Ca^{2+}]_i$ change

When 100 μM-ATP, 100 μM-ADP or 1 mM-GTP was added to the Ca^{2+}-free cell suspension (with 0.5 mM-EGTA), the $[Ca^{2+}]_i$ rapidly increased to about the same level as that observed in the presence of 1.3 mM extracellular Ca^{2+}. Then it decreased rapidly to a level below the prestimulated value (Figs. 5*a*–5*c*; Table 1), indicating that the initial rise in $[Ca^{2+}]_i$ is due to Ca^{2+} mobilization from intracellular pools.

Effects of Ca^{2+}-channel blocker

La^{3+} is a non-selective Ca^{2+}-channel antagonist and has been reported to inhibit receptor-mediated Ca^{2+} entry from the extracellular spaces in various types of cells [25–27]. When 100 μM-$LaCl_3$ was added at the plateau under ATP stimulation, $[Ca^{2+}]_i$ gradually decreased and reached a level below the

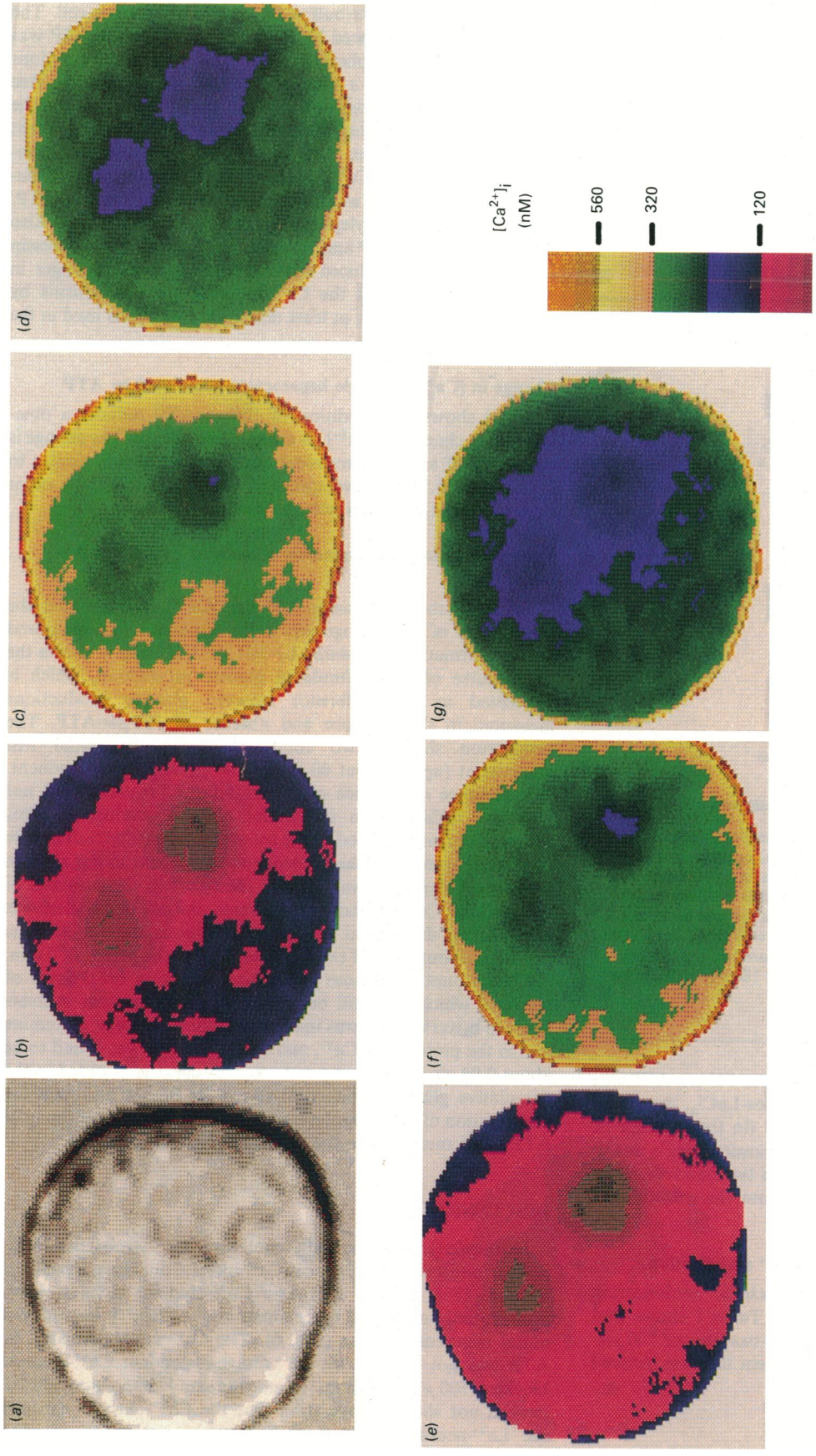

Fig. 7. Imaging of the distribution of fura-2 in a single hepatocyte

Microscopic images of fura-2 fluorescence were saved in a SIT-camera and analysed by a Spex imaging system at 25 °C. (*a*) Bright-field picture of the hepatocyte; (*b*)–(*g*) fluorescence distribution images at various times before or after stimulation with the agonist: *b*, resting; *c* and *d* are taken 7 s and 30 s after the addition of 100 μM-ATP respectively; *e*, 5 min after washing with agonist-free medium; *f* and *g* are taken 7 s and 30 s after addition of 10 nM-vasopressin. The bar at the bottom indicates 10 μm. The coloured strip indicates the scale of relative intensity of the ratio of fura-2 fluorescence and corresponding $[Ca^{2+}]_i$.

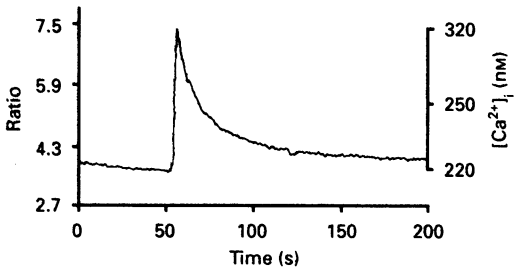

Fig. 8. Change in $[Ca^{2+}]_i$ in a single hepatocyte stimulated by 100 μM-ATP

Typical data at 25 °C are shown.

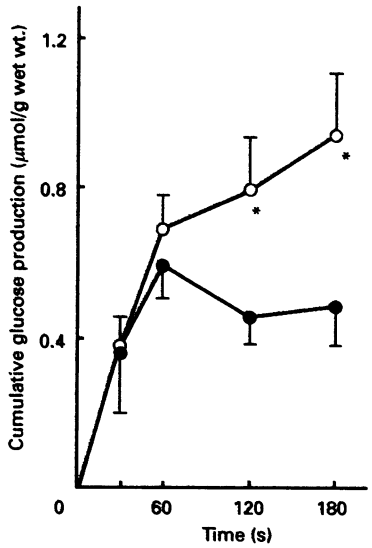

Fig. 9. Time-dependent activation of gluconeogenesis with 100 μM-ATP

At zero time, 100 μM-ATP was added into hepatocyte suspensions to stimulate glucose production in the absence (●) or presence (○) of 1.3 mM extracellular Ca^{2+}. The value on the ordinate is the cumulative production of glucose stimulated by ATP, which is calculated as the difference between values measured in the presence and absence of ATP. Values are means ± S.E.M. (μmol/g wet wt.) from 7–10 cell preparations: * $P < 0.05$ between values measured in the presence and absence of extracellular Ca^{2+} at 120 s and 180 s (t statistic for two means).

prestimulated value within 60 s (Fig. 6*a*). When 100 μM-ATP was added to the cells in the presence of 100 μM-$LaCl_3$, the initial transient increase was not affected by La^{3+} (in the presence of 1.3 mM-Ca^{2+}) (Fig. 6*b*), indicating that the transient rise is due to Ca^{2+} release from the intracellular pools and the maintenance of the plateau level needs the Ca^{2+} supply from the extracellular medium.

Effects of various drugs on intracellular Ca^{2+} mobilization

We used several agents that inhibit or quench Ca^{2+} mobilization from the intracellular Ca^{2+} pools [28–30]. Table 1 shows that pretreatment with 40 mM-caffeine, 2 mM-oxalate or 60 μM-dantrolene sodium inhibits the initial transient increase induced by ATP, ADP and GTP by 50–70 %.

Distribution of $[Ca^{2+}]_i$ in single cells

The distribution of the intracellular Ca^{2+} in single hepatocytes was obtained by measuring the fluorescence intensity of fura-2 under a microscope. Fig. 7(*a*) shows a bright-field picture (Nomarski) of a single hepatocyte. This cell has two nuclei. Figs. 7(*b*)–7(*g*) show the distribution of $[Ca^{2+}]_i$ in the same cell. The increase in $[Ca^{2+}]_i$ induced by the addition of 100 μM-ATP was more rapid in the peripheral regions than in the central regions of the cell (Fig. 7*c*) (7 s after stimulation). After 30 s, the free $[Ca^{2+}]_i$ decreased to a level that is higher than the control, and the distribution became homogeneous throughout the cell, except the region of the nucleus (Fig. 7*d*). Figs. 7(*e*)–7(*g*) show a time-dependent change in $[Ca^{2+}]_i$ induced by stimulation with 10 nM-vasopressin. The result was quite similar to that induced by ATP. Effects of 10 μM-phenylephrine (results not shown) were also similar to those of ATP and vasopressin. Thus ATP, vasopressin and phenylephrine induced similar time-dependent changes in $[Ca^{2+}]_i$, indicating that the Ca^{2+}-mobilization mechanisms by these agents are similar, at least under the conditions used in the present study.

Change in $[Ca^{2+}]_i$ in single hepatocytes stimulated by ATP

Fig. 8 shows that addition of 100 μM-ATP induces a time-dependent change in $[Ca^{2+}]_i$ in a single hepatocyte. The change is composed of an initial transient peak and a plateau, similar to Figs. 1 and 4. Repetitive spikes in $[Ca^{2+}]_i$, as found by other researchers [31,32], were not observed.

Time courses of gluconeogenesis stimulated by ATP in the initial stage

To study the relationship between $[Ca^{2+}]_i$ changes and the stimulation of gluconeogenesis from glutamine, we measured glucose formation stimulated by 100 μM-ATP. Fig. 9 shows the time course of ATP-stimulated glucose production, which is calculated as the difference between glucose productions measured in the presence and absence of 100 μM-ATP. The production showed two components, i.e. the initial fast component (up to about 60 s) and the subsequent component. The presence or absence of extracellular 1.3 mM-Ca^{2+} did not give any difference in the initial glucose production. This component corresponded to the transient rise in $[Ca^{2+}]_i$. The rate of gluconeogenesis of the subsequent component in the absence of extracellular Ca^{2+} was smaller than that in the presence of extracellular Ca^{2+}. In these experiments, the cell population was about 4.3 mg dry wt./ml. Under the conditions, the ecto-ATPase degraded about 75 % of extracellular ATP in the period of 3 min.

The amount of glucose production owing to breakdown of glycogen which may still be present in small amounts in livers from 48 h-starved rats was measured in the absence of glutamine and in the presence of Ca^{2+}, and the ATP effect was found to be about 0.04 μmol/min per g wet wt. This effect is included in the cumulative glucose production shown in Fig. 9, although the contribution of glycogenolysis was less than 10–20 % of the total ATP effect measured in the presence of glutamine.

DISCUSSION

Extracellular ATP initially mobilizes Ca^{2+} from the intracellular pools and then induces Ca^{2+} influx from the extracellular medium (Fig. 1). An inorganic Ca^{2+}-channel blocker, La^{3+}, preferentially abolished the plateau level of $[Ca^{2+}]_i$ but not the initial transient increase (Fig. 6). The Ca^{2+} entry activated by ATP was not blocked by the voltage-dependent Ca^{2+}-channel blockers 100 μM-diltiazem, 10 μM-verapamil or 5 μM-nifedipine (results not shown), indicating that the Ca^{2+} entry is through the La^{3+}-sensitive voltage-insensitive channel in the plasma membrane. Moreover, the La^{3+}-sensitive Ca^{2+} channel was not involved in the maintenance of $[Ca^{2+}]_i$ in the resting state of cells,

since the control value was not affected by the addition of La^{3+} (Fig. 6*b*).

We examined the source of the initial rapid Ca^{2+} increase mediated by P_2-purinergic stimulation in hepatocytes. In the experiments, we used several drugs. Caffeine causes Ca^{2+}-induced Ca^{2+} release from the sarcoplasmic (SR) and endoplasmic reticulum (ER) and finally depletes the stored Ca^{2+} in many cell species [29]. Oxalate is assumed to inhibit Ca^{2+} release by stimulating Ca^{2+} uptake by SR and ER [30]. Dantrolene sodium is known to inhibit Ca^{2+} releases from SR and ER by trapping Ca^{2+} [28]. The present rapid increases in $[Ca^{2+}]_i$ by ATP, ADP and GTP were preferentially suppressed by these inhibitors (Table 1), indicating that these P_2-purinergic agonists activate Ca^{2+} efflux from the ER.

In the present study, digital imaging fluorescence microscopy of fura-2-loaded hepatocytes was also used to examine changes in the distribution of $[Ca^{2+}]_i$ in single cells in response to receptor activation by P_2-purinergic agonists.

The initial rapid increase in $[Ca^{2+}]_i$ by ATP was greater in the peripheral parts than the central parts of the cell. Similar changes in $[Ca^{2+}]_i$ were also caused by vasopressin (Fig. 7) and phenylephrine. The initial rise in $[Ca^{2+}]_i$ in the periphery of the cell could not be localized to a specific region of the periphery. This might be due to loss of asymmetric metabolic functions and functional depolarization of hepatocytes during isolation and storage [33].

As seen in Figs. 7(*b*)–7(*g*), the $[Ca^{2+}]$ at the edge of the cell is apparently higher than that in the rest of the cell. For this reason, a computational error of $[Ca^{2+}]$ at the boundary between the medium and the cell membrane is considered. But apparently this is not the sole reason. The thickness of the thin high-$[Ca^{2+}]$ zone at the edge was not constant: that is, the thickness measured when $[Ca^{2+}]_i$ increased in the peripheral region (Figs. 7*c* and 7*f*) is larger than that measured when $[Ca^{2+}]_i$ decreased (Figs. 7*d* and 7*g*). This change in $[Ca^{2+}]$ at the edge may be understood from an analogous change in water height where gushing water strikes a wall and then the water recedes. The other possibility is the extracellular Ca^{2+} influx accumulating under the plasmalemma. But the high-$[Ca^{2+}]$ zone was also found in the absence of extracellular Ca^{2+}. Further study is necessary to determine the correct reason for the appearance of the high-$[Ca^{2+}]$ edge zone.

Repetitive $[Ca^{2+}]_i$ spikes have been found in single hepatocytes stimulated by 0.5–3 μM-ATP measured with aequorin [31] and fura-2 [32]. Here we could not find them (Fig. 8). The most plausible reason for this is that we used a very high concentration of ATP (100 μM). It is relevant to refer to the previous findings by Woods *et al.* [34] that very high concentrations of vasopressin (> 10 nM) induced a rise in $[Ca^{2+}]_i$ followed by a slow decay and that intermediate (1.5 nM) and low (< 1 nM) vasopressin concentrations induced repetitive $[Ca^{2+}]_i$ spikes. On the other hand, other researches [35,36] have suggested that primary culture of hepatocytes is important for observing $[Ca^{2+}]$ oscillations in single hepatocytes, since the agonist-induced $[Ca^{2+}]_i$ oscillations need functional repolarization of hormone receptors/signal-transduction elements during culture.

The rapid hormonal stimulation of hepatic glucose formation, including glycogenolysis, is mediated by two distinct mechanisms, involving either cyclic AMP or Ca^{2+}. The following results presented here show that the $[Ca^{2+}]_i$ elevation is closely associated with gluconeogenesis from glutamine. (1) The time course of glucose production had two components, in accordance with that of $[Ca^{2+}]_i$ elevation. In the first phase shown in Fig. 9 (up to 60 s), the rate of glucose syntheses was fast (about 0.70 μmol/min per g wet wt). The rate in the second phase in the presence of extracellular Ca^{2+} was slow (about 0.1 μmol/min per g wet wt.). (2) The first phase of glucose syntheses did not depend on the presence or absence of extracellular Ca^{2+} (Fig. 9). Corresponding to this fact, the rapid transient rise in $[Ca^{2+}]_i$ did not depend on the extracellular Ca^{2+} (Fig. 5). The second phase of glucose synthesis markedly slowed down in the absence of extracellular Ca^{2+}. Therefore, gluconeogenesis from glutamine was triggered by the initial transient rise in $[Ca^{2+}]_i$ even in the absence of extracellular Ca^{2+}. It is suggested that both the initial transient rise in $[Ca^{2+}]_i$ and the maintenance of the plateau level play important roles for hepatic gluconeogenesis.

Gluconeogenesis from glutamine includes multi-enzymic steps, and the initial event is an ammonia-activation of glutaminase. In the present study we did not determine what step is rate-determining for glucose production under the present conditions. If the rate-determining step is ammonia accumulation induced by ATP, simultaneous observation of the distribution of the intracellular pH in single hepatocytes together with the distribution of $[Ca^{2+}]_i$ will be an interesting future work.

This work was partly supported by grants from the Ministry of Education, Science and Culture of Japan.

REFERENCES

1. Gordon, J. L. (1986) Biochem. J. **233**, 309–319
2. Buxton, D. B., Robertson, S. M. & Olson, M. S. (1986) Biochem. J. **237**, 773–780
3. Dewitt, L. M. & Putney, J. W., Jr. (1983) FEBS Lett. **160**, 259–263
4. Haussinger, D., Stehle, T. & Gerok, W. (1987) Eur. J. Biochem. **167**, 65–71
5. Keppens, S. & DeWulf, H. (1985) Biochem. J. **231**, 797–799
6. Krell, H., Jaeschke, H. & Pfaff, E. (1985) Biochem. Biophys. Res. Commun. **131**, 139–145
7. Okajima, F., Tokumitsu, T., Kondo, Y. & Ui, M. (1987) J. Biol. Chem. **262**, 13483–13490
8. Staddon, J. M. & McGivan, J. D. (1985) Eur. J. Biochem. **151**, 567–572
9. Guinzberg, R., Laguna, I., Zentella, A., Guzman, R. & Pina, E. (1987) Biochem. J. **245**, 371–374
10. Charest, R., Blackmore, P. F. & Exton, J. H. (1985) J. Biol. Chem. **260**, 15789–15794
11. Horstmann, D. A., Tennes, K. A. & Putney, J. W., Jr. (1986) FEBS Lett. **204**, 189–192
12. Keppens, S. & DeWulf, H. (1986) Biochem. J. **240**, 367–371
13. Williamson, J. R., Cooper, R. H., Joseph, S. K. & Thomas, A. P. (1985) Am. J. Physiol. **248**, C203–C216
14. Berry, M. N. & Friend, D. S. (1969) J. Cell Biol. **43**, 506–520
15. Cornell, N. W., Lund, P., Hems, R. & Krebs, H. A. (1973) Biochem. J. **134**, 671–672
16. Krebs, H. A. & Henseleit, K. (1932) Hoppe-Seyler's Z. Physiol. Chem. **210**, 33–66
17. Cobbold, P. H. & Rink, T. J. (1987) Biochem. J. **248**, 313–328
18. Grynkiewicz, G., Poenie, M. & Tsien, R. Y. (1985) J. Biol. Chem. **260**, 3440–3450
19. Malgaroli, A., Milani, D., Meldolesi, J. & Pozzan, T. (1987) J. Cell Biol. **105**, 2145–2155
20. Kashiwagura, T., Erecinska, M. & Wilson, D. F. (1985) J. Biol. Chem. **260**, 407–414
21. Bergmeyer, H. U., Bernt, E., Schmidt, F. & Stock, H. (1974) in Methods of Enzymatic Analysis (Bergmeyer, H. U., ed.), vol. 4, pp. 1196–1201, Verlag Chemie/Academic Press, New York, San Francisco and London
22. Lamprecht, W. & Trautschold, I. (1974) in Methods of Enzymatic Analysis (Bergmeyer, H. U., ed.), vol. 4, pp. 2101–2110, Verlag Chemie/Academic Press, New York, San Francisco and London
23. Gordon, E. L., Pearson, J. D., Dickinson, E. S., Moreau, D. & Slakey, L. L. (1989) J. Biol. Chem. **264**, 18986–18992
24. Lin, S. H. (1989) J. Biol. Chem. **264**, 14403–14407
25. Andersson, T., Dahlgen, C., Possan, T., Stendahl, O. & Lew, P. D. (1986) Mol. Pharmacol. **30**, 437–443
26. Aub, D. L., McKinney, J. S. & Putney, J. W., Jr. (1982) J. Physiol. (London) **331**, 557–565
27. Pandol, S. J., Schoeffield, M. S., Fimmel, C. J. & Muallem, S. (1987) J. Biol. Chem. **262**, 16963–16968

28. Donowitz, M. (1983) Am. J. Physiol. **245**, G165–G177
29. Moore, L. & Pastan, I. (1977) J. Cell. Physiol. **91**, 289–296
30. Ponnappa, B. C., Dormer, R. L. & Williams, J. A. (1981) Am. J. Physiol. **240**, G122–G129
31. Dixon, C. J., Woods, N. M., Cuthbertson, K. S. R. & Cobbold, P. H. (1990) Biochem. J. **269**, 499–502
32. Kawanishi, T., Blank, L. M., Harootunian, A. T., Smith, M. T. & Tsien, R. Y. (1989) J. Biol. Chem. **264**, 12859–12866
33. Maurice, M., Rogier, E., Cassio, D. & Feldman, G. (1988) J. Cell Sci. **90**, 79–92
34. Woods, N. M., Cuthbertson, K. S. R. & Cobbold, P. H. (1986) Nature (London) **319**, 600–602
35 Monck, J. R., Reynolds, E. E., Thomas, A. P. & Williamson, J. R. (1988) J. Biol. Chem. **263**, 4569–4575
36. Rooney, T. A., Renard, D. C., Sass, E. J. & Thomas, A. P. (1991) J. Biol. Chem. **266**, 12272–12282

Received 15 May 1991/11 November 1991; accepted 21 November 1991